J. Biochem. **143**, 297–304 (2003)
DOI: 10.1093/jb/mvg143

Structure of the Transition State Analog of Medium-Chain Acyl-CoA Dehydrogenase. Crystallographic and Molecular Orbital Studies on the Charge-Transfer Complex of Medium-Chain Acyl-CoA Dehydrogenase with 3-Thiaoctanoyl-CoA

Atsuko Satoh[1], Yoshitaka Nakajima[1], Ikuko Miyahara[1], Ken Hirotsu[*,1], Takeyuki Tanaka[2], Yasuzo Nishina[3], Kiyoshi Shiga[3], Haruhiko Tamaoki[4], Chiaki Setoyama[4] and Retsu Miura[*,4]

[1]Department of Chemistry, Graduate School of Science, Osaka City University, Sumiyoshi-ku, Osaka 558-8585; [2]Department of Life Science, Graduate School of Science and Technology, Kobe University, Nada-ku, Kobe 657-8501; and Departments of [3]Molecular Physiology and [4]Molecular Enzymology, Graduate School of Medical Sciences, Kumamoto University, Honjo, Kumamoto 860-0811

Received May 8, 2003; accepted June 17, 2003

The flavoenzyme medium-chain acyl-CoA dehydrogenase (MCAD) eliminates the α-proton of the substrate analog, 3-thiaoctanoyl-CoA (3S-C8-CoA), to form a charge-transfer complex with deprotonated 3S-C8-CoA. This complex can simulate the metastable reaction intermediate immediately after the α-proton elimination of a substrate and before the β-hydrogen transfer as a hydride, and is therefore regarded as a transition-state analog. The crystalline complex was obtained by co-crystallizing MCAD in the oxidized form with 3S-C8-CoA. The three-dimensional structure of the complex was solved by X-ray crystallography. The deprotonated 3S-C8-CoA was clearly located within the active-site cleft of the enzyme. The arrangement between the flavin ring and deprotonated 3S-C8-CoA is consistent with a charge transfer interaction with the negatively charged acyl-chain of 3S-C8-CoA as an electron donor stacking on the pyrimidine moiety of the flavin ring as an electron acceptor. The structure of the model complex between lumiflavin and the deprotonated ethylthioester of 3-thiabutanoic acid was optimized by molecular orbital calculations. The obtained theoretical structure was essentially the same as that of the corresponding region of the X-ray structure. A considerable amount of negative charge is transferred to the flavin ring system to stabilize the complex by 9.2 kcal/mol. The large stabilization energy by charge transfer probably plays an important role in determining the alignment of the flavin ring with 3S-C8-CoA. The structure of the highest occupied molecular orbital of the complex revealed the electron flow pathway from a substrate to the flavin ring.

Key words: charge-transfer complex, flavoenzyme, medium-chain acyl-CoA dehydrogenase, molecular orbital calculation, three-dimensional structure, X-ray crystallography.

Abbreviations: C8-CoA, octanoyl-CoA; ETF, electron-transferring flavoprotein; HOMO, highest occupied molecular orbital; MCAD, medium-chain acyl-CoA dehydrogenase; rms, root mean square; 3S-C8-CoA, 3-thiaoctanoyl-CoA.

Acyl-CoA dehydrogenases comprise a family of FAD-dependent flavoenzymes that catalyze the initial and rate-limiting step, *i.e*., the dehydrogenation of acyl-CoA to yield *trans*-2-enoyl-CoA, of the mitochondrial fatty acid β-oxidation pathway; each member of the family shows distinct substrate specificity in terms of the length and shape of the acyl-chain (*1*, *2*). Medium-chain acyl-CoA dehydrogenase (MCAD), which is active toward acyl-CoAs with acyl-chains C4 to C12 and has the highest activity with C8, is the most extensively investigated member of the family and has been regarded as the prototype of the family. Kim *et al*. have reported the three-dimensional structure of MCAD with and without substrate and described the substrate recognition mode (*3*). However, judging from the reactivity of MCAD with octanoyl-CoA and the conditions they employed for crystallographic data collection, the reported crystal structure of MCAD with substrate may not correspond to the enzyme-substrate complex, but rather appears most likely to represent the reduced enzyme-product complex, possibly with marginal contributions of the oxidized enzyme–substrate complex and reduced enzyme-substrate complex.

During the dehydrogenation of an acyl-CoA catalyzed by members of the acyl-CoA dehydrogenase family, the α-hydrogen in the acyl moiety is abstracted as a proton by a protein base, *i.e.*, Glu-COO^-, and the β-hydrogen is transferred as a hydride to the N(5) of flavin (*2*). Ghisla *et al*. proposed that the two hydrogen-removal processes are

*To whom correspondence should be addressed. E-mail: hirotsu@sci.osaka-cu.ac.jp, Fax: +81-66-605-3131(K. Hirotsu) or miura@gpo.kumamoto-u.ac.jp, Fax: +81-96-373-5066 (R. Miura).

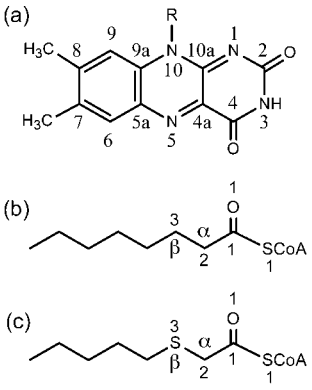

Fig. 1. **The structure and numbering system of the flavin ring of FAD (a), octanoyl-CoA (b), and 3S-C8-CoA (c).**

concerted in the MCAD-catalyzed dehydrogenation on the basis of the deuterium isotope effect with substrate deuterated at C(2) and C(3) of acyl-CoA (*4*). However, the two processes proceed either in a concerted or stepwise manner with α-proton abstraction preceding β-hydride transfer depending on the member of the family, type of substrate, or pH of the medium (*2*). According to the reaction mechanism based on substrate recognition as deduced from the crystallographic studies of MCAD (*3*), the substrate C(1)-carbonyl oxygen is hydrogen-bonded with the ribityl-2′-hydroxyl group of FAD and the backbone N-H of Glu376 (*3*), and these hydrogen bonds are critical not only for substrate-recognition but especially for substrate-activation in lowering the p*K*a value of the substrate α-proton. Thorpe and coworkers first reported the interaction between 3-thiaacyl-derivatives of acyl-CoA and MCAD, and demonstrated that complexes of these ligands with MCAD exhibit a characteristic broad and strong absorption band in the long wavelength region (*5*). The 3-thiaacyl-CoAs are unique substrate analogs in that they possess the α-proton to be abstracted by the catalytic base, *i.e.*, Glu376-COO^-, but lack the β-hydride, which would otherwise be transferred to the flavin N(5)-position (see Fig.1 for the flavin numbering system and the structure of 3-thiaoctanoyl-CoA). As a result, when 3-thiaacyl-CoA is bound to MCAD, it undergoes α-proton abstraction by Glu376-COO^- and the anionic form of the ligand forms a charge-transfer complex with flavin instead of reducing the flavin by β-hydride transfer. More specifically, in the reaction between 3-thiaacyl-CoA and MCAD, the complex freezes at the stage after α-proton abstraction in the form of a charge-transfer state. The complex, therefore, simulates the metastable intermediate during α-proton abstraction and β-hydride transfer in the catalysis of MCAD with a natural substrate. Thus, the 3-thiaoctanoyl-CoA-MCAD complex is regarded as a transition-state analog. Among straight-chain 3-thiaacyl-CoAs, 3-thiaoctanoyl-CoA (3S-C8-CoA) forms a complex with MCAD, exhibiting the most intense charge-transfer band at 808 nm, and the complex consists exclusively of the charge-transfer complex between the anionic ligand and oxidized flavin, while complexes of 3-thiaacyl-CoA with shorter or longer chain-lengths than C8 comprise fractions of other species in addition to the charge-transfer complex (*6*). In this report we present the crystallographic analysis of the 3S-C8-CoA-MCAD complex and discuss the conformation of the ligand, the recognition mode of the ligand by the enzyme, and the mutual positioning between the ligand and flavin with reference to the reaction mechanism and particularly the transition state during the reductive half-reaction of MCAD. The charge-transfer nature of the complex between the anionic 3-thiaoctanoyl moiety and the flavin ring in the crystal structure was substantiated by the density functional theory molecular orbital calculations and the stabilization energy of the complex by the charge-transfer interaction was estimated.

Table 1. **Crystallographic data set for 3S-C8-CoA-MCAD.**

Space group	$P2_12_12_1$, No. 19
Cell constant (Å)	
a	99.0
b	110.6
c	147.8
Temperature (K)	287
Wavelength (Å)	1.00
Resolution range (Å)	50.0–2.4 (2.49–2.40)[a]
No. of reflections	
Observation	201,618
Unique	53,947 (4,381)[a]
Completeness (%)	84.1 (69.5)[a]
R_{merge}[a] (%)	5.7 (20.9)[a]
R_{factor} (%)	19.7 (27.8)[a]
R_{free}[c] (%)	25.9 (33.9)[a]
Deviations	
Bond lengths (Å)	0.008
Bond angles (deg)	1.347
Dihedral angles (deg)	21.252
Improper torsion angles (deg)	0.876
Mean B factors	
Main chain atoms (Å^2)	27.6
Side chain atoms (Å^2)	28.4
Hetero atoms (Å^2)	29.1
Water molecules (Å^2)	32.2

[a]The values in parentheses are for highest resolution shells. [b]$R_{merge} = \Sigma_{hkl} \Sigma_i |I_{hkl,i} - \langle I_{hkl} \rangle| / \Sigma_{hkl} \Sigma_i I_{hkl,i}$, where I = observed intensity and $\langle I \rangle$ = average intensity for multiple measurements. [c]Free R was calculated using 10% randomly selected reflections.

MATERIALS AND METHODS

Crystallization and Data Collection—Medium-chain acyl-CoA dehydrogenase (MCAD) was purified from pig kidney as described previously (*7*, *8*). Crystallization of MCAD in complex with 3S-C8-CoA was performed using the hanging-drop vapor diffusion method at 277K (*9*), with a protein solution (7–8 mg protein/ml, 10 mM Tris-acetate, pH 7.0) and a reservoir solution [10–14% (w/v) PEG4000, 10 mM Tris-acetate, pH6.0]. When an excess amount of 3S-C8-CoA was added to the protein solution, the solution changed from yellow to yellowish-green and the yellowish-green complex of 3S-C8-CoA-MCAD was obtained as a new form of the space group $P2_12_12_1$ with one tetramer per asymmetric unit corresponding to a specific volume V_m = 2.15 Å^3/Da and solvent content of 33% (*10*). The data set for the complex crystal was collected to

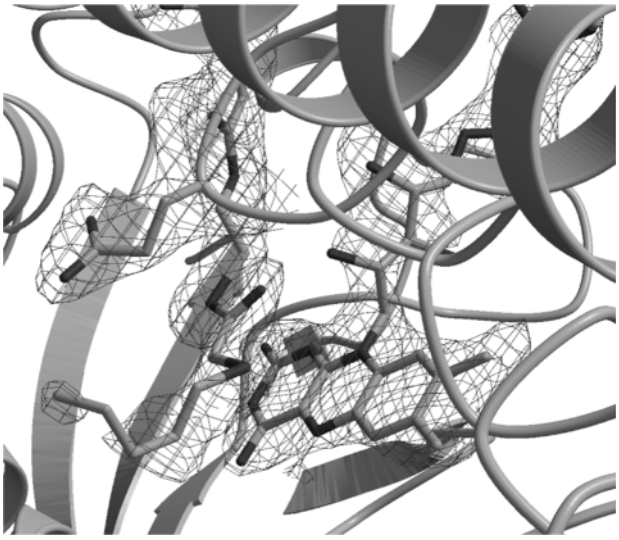

Fig. 2. **The $2F_o$–F_c electron density map of 3S-C8-CoA-MCAD calculated using 10.0–2.3 Å resolution for FAD and 3S-C8-CoA.**

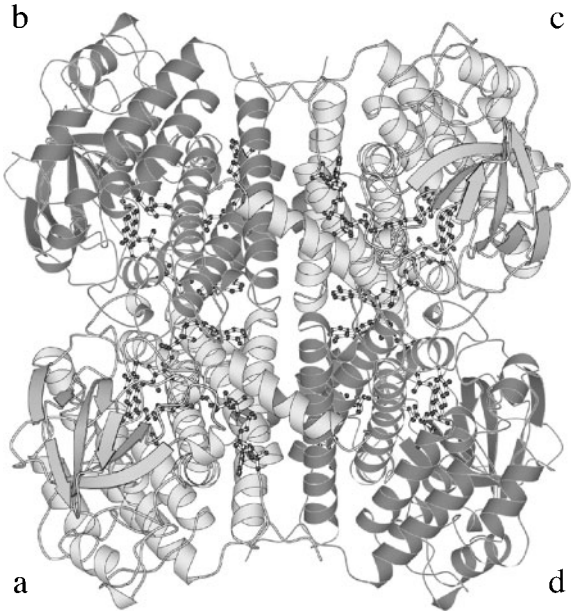

Fig. 3. **Cα ribbon tracings of the MCAD complex with 3S-C8-CoA viewed down from a molecular 2-fold axis.** FAD and 3S-C8-CoA, shown by the ball-and-stick model, are bound to the large crevice. The dimer unit comprises subunits a and b (or d and c) and its two-fold axis is parallel to the horizontal axis.

2.4 Å at 293 K on the BL18 station at Photon Factory (Tsukuba). The data were processed and scaled with the programs DENZO and SCALEPACK (*11*) (Table 1).

Structure Refinement—The structure of 3S-C8-CoA-MCAD in the space group $P2_12_12_1$ was solved by the molecular replacement method (*12*) using the previously determined structure of MCAD in the space group $C222_1$ with one tetramer per asymmetric unit (*3*, *13*). The initial refinement of the structure by simulated annealing and energy minimization with noncrystallographic 222 symmetry for the tetramer reduced the R_{factor} and R_{free} to 21.4 and 25.8%, respectively, using the reflections between 50.0 and 2.4 Å (*14*). After each round of refinement, the model was refitted to the omit electron density map by the program O (*15*). The difference Fourier map exhibited a long and continuous electron density corresponding to the anionic 3S-C8-CoA. The 2*F*o-*F*c electron density map for the anionic 3S-C8-CoA is shown in Fig. 2. The model of anionic 3S-C8-CoA with the planar group S1, C1, O1, C2, and S3 atoms fitted well to the map. The restraint on the noncrystallographic symmetry was removed and water molecules were picked up on the basis of the peak height and the distance criteria from the difference maps. Further model building and refinement cycles resulted in an R_{factor} of 19.7% and R_{free} of 25.9% with the reflection data between 50.0–2.4 Å. The maximum temperature factor of the assigned water molecules was 57.6 Å^2 (Table 1).

Quality of the Structure—The refined model of the 3S-C8-CoA-MCAD complex contained 1,540 amino acid residues for three subunits, 1,538 amino acid residues for one subunit, and four FAD molecules with 318 water molecules. No interpretable electron density was observed for ten N-terminal residues in each of the four subunits and two C-terminal residues in one of the four subunits. The analysis of the stereochemistry with PROCHECK (*16*) showed that the model had a good quality with 90.7% of residues in the most favored region of the Ramachandran plot, 9.2% in the additionally allowed region, and 0.2% in the generously allowed region. Structure diagrams were drawn with the programs Molscript (*17*), Bobscript (*18*), and Raster3D (*19*).

Molecular Orbital Calculations—All calculations were performed with the Gaussian98 program (*20*) on the HP Exemplar Technical Server V2250K and the Dell Precision Workstation 450 machines. Lumiflavin was adopted as a model of flavin, and the anionic ligand was designed by removal of the α-proton of the ethylthioester of 3-thiabutanoic acid which embodies the reaction site of 3S-C8-CoA. The complex between lumiflavin and the anionic ligand was modeled in such a way that the ligand approaches lumiflavin with reference to the coordinates of the corresponding atoms in the X-ray structure. The complex was optimized with respect to all geometrical parameters using the B3LYP density functional and 6–311+G(2d,p) basis set (*21*, *22*) with the closed-shell system. The spatial arrangement between lumiflavin and the anionic ligand in the optimized complex model was investigated by least squares fitting to the X-ray structures determined herein. The amount of transferred charge was estimated from the atomic charges by Mulliken population analysis (*23*, *24*). Drawings of all molecular orbitals were produced using Chem3D Pro software (Cambridge Software, UK) on the basis of the cube files obtained from the Gaussian98 program. The values of the isocontour parameters were set to 0.035 atomic unit.

RESULTS AND DISCUSSION

Description of the Structure—MCAD in complex with 3S-C8-CoA is folded into a tetrameric form with a noncrystallographic 222 symmetry (Fig. 3). The backbone atoms of the four subunits are superimposed on one another with rms deviations of 0.269–0.437 Å by the

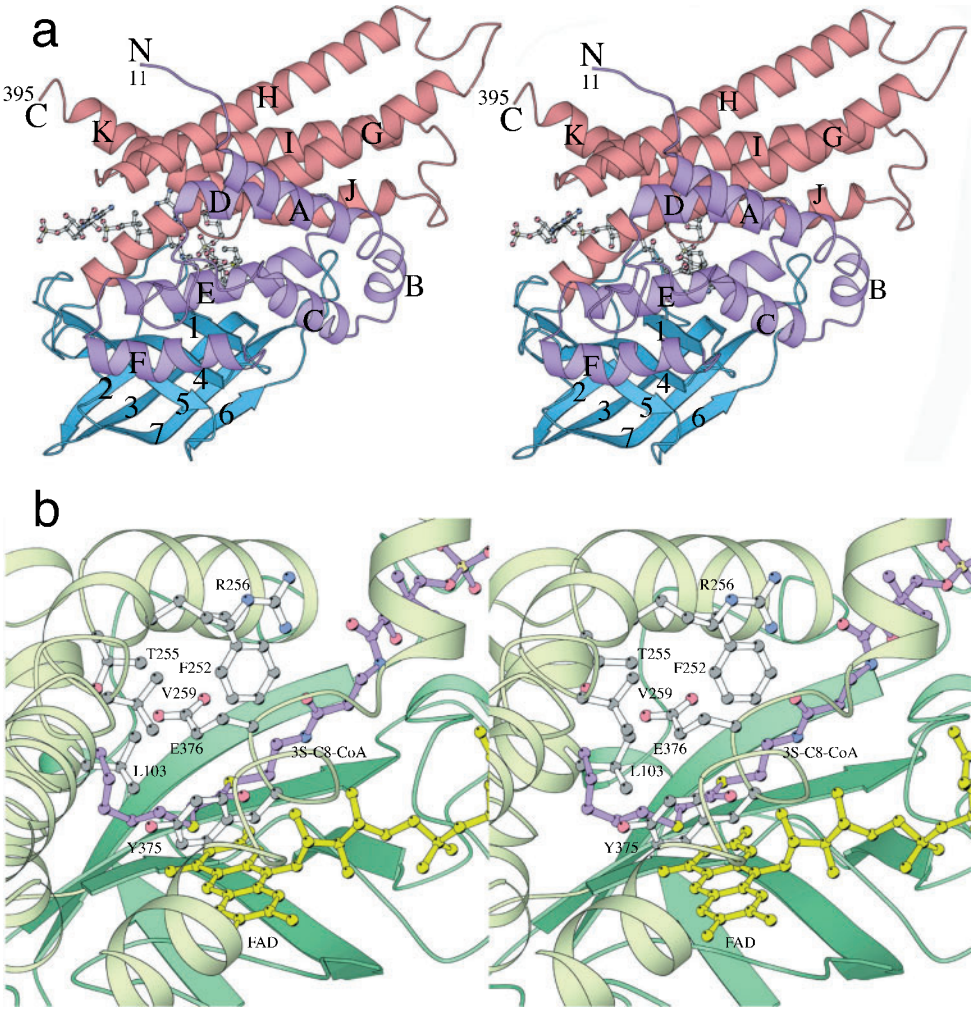

Fig. 4. **(a) Stereoview of a subunit of the 3S-C8-CoA-MCAD structure with secondary structure assignments.** α-Helices are denoted as A–F in the N-terminal α-domain (green), and G–L in the C-terminal α-domain (light purple). β-Strands are denoted as 1–7 in the β-domain (blue). The cofactor FAD and 3S-C8-CoA are represented by the ball-and-stick model. **(b) Stereoview of the active site in 3S-C8-CoA-MCAD.** The β-domain and N-terminal α-domain are shown as pale gray and green ribbons, respectively. The active site residues, FAD (yellow) and 3S-C8-CoA (light purple) are represented by ball-and-stick models.

least-squares method, indicating that all the subunits of MCAD are folded into the same structure. One subunit in the tetramer interacts with the other three subunits and the surface areas of subunit interfaces are 1,676 for a and b, 1,645 for a and d, and 475 Å^3 for a and c subunits. The tetramer may be considered to be the assembly of two functional dimers (a and b, and c and d in Fig. 3) around a 2-fold axis since FAD interacts with subunits a and b or subunits c and d (*3*). The Cα atoms of the functional dimer units in the 3S-C8-CoA-MCAD complex were superimposed onto the corresponding ones in the native MCAD and the C8-CoA-MCAD complex with rms deviations of 0.385 and 0.437 Å, respectively, indicating that the dimer units in different crystallographic environments have quite similar conformations (*3*).

The subunit is divided into the N-terminal α-domain (N-terminus to Leu129), β-domain (Met130 to Gly239), and C-terminal α-domain (Glu240 to C-terminus) (Fig. 4a). The β-domain is located between the N-terminal α-domain and the C-terminal α-domain interconnecting these two domains. The N- and C-terminal α-domains pack together, apparently forming a single α-domain. The N-terminal α-domain consists of five α-helices (A–F) with the antiparallel α-helices A, C, D, and E forming a pseudo four-helix-bundle structure. α-Helix E forms a part of the active-site crevice for binding the fatty acyl chain of a substrate. The β-domain is made up of a three-stranded β-sheet (*1*, *4*, and *5*) and an antiparallel four-stranded β-sheet (*2*, *3*, *7*, and *6*). The C-terminal α-domain consists of six α-helices (G–L). The α-helices G, H, I, and K form a four-helix bundle with the short α-helix J between α-helices I and K. The binding sites for FAD and 3S-C8-CoA are mainly formed at the interface between the β-domain and the C-terminal α-domain.

FAD and 3S-C8-CoA Binding—When the α-carbon atoms of the 3S-C8-CoA-MCAD dimer unit are fitted onto the corresponding α-carbon atoms of C8-CoA-MCAD (*3*), the FADs in both complexes are superimposable, although the flavin rings show a slight and parallel shift of about 0.3 Å along N5-N10 of FAD. The location of 3S-C8-CoA bound to the subunit a, c or d is essentially the same as that of C8-CoA except for 3S-C8-CoA liganded to subunit b. The adenosine 3′-phosphate moiety of 3S-C8-CoA in subunit b is approached by Arg123 of subunit c in the neighboring tetramer unit. The Arg123 occupies a part of the binding site for adenosine 3′-phosphate and interacts with the 3′-phosphate group, inducing a positional shift of 3S-C8-CoA from the location observed in the other three subunits. We use the orientation of 3S-C8-CoA in the subunit a, c or d as the reference in the following discussion, since the location of 3S-C8-CoA in sub-

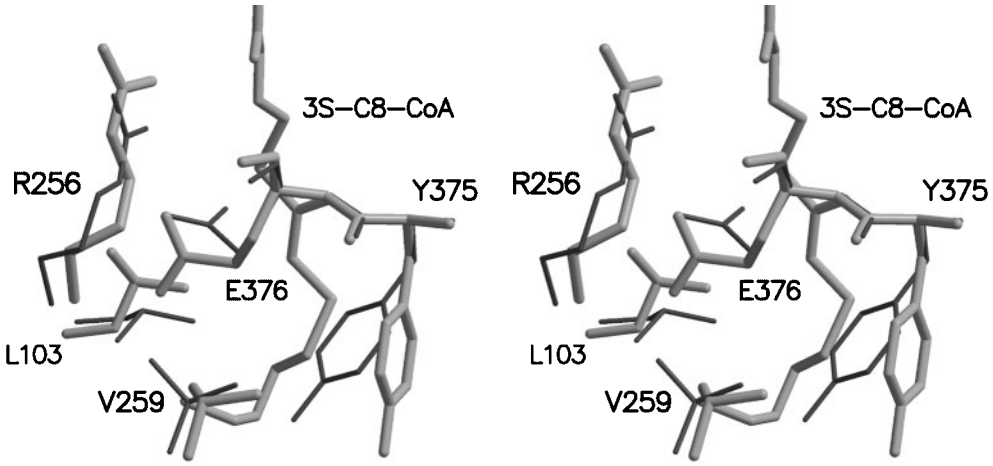

Fig. 5. **Side-chain movement of Arg256 and Glu376 upon complex formation.** Thin and thick lines correspond to the native (*3*) and complex forms of the enzyme, respectively.

unit b is affected by artifactual crystallographic artifactual intermolecular interactions.

FAD interacts with the residues from one dimer unit of the tetramer except for one hydrogen bond between the adenine group of FAD and a glutamate of the other dimer unit. The riboflavin moiety of FAD is bound to the crevice between the β-domain and the C-terminal α-domain with the *si*-face of the flavin ring oriented toward the β-domain as observed in C8-CoA-MCAD (*3*) (Fig. 4b). The pyrophosphate part of FAD interacts with the β-domain and the C-terminal α-domain of the other subunit of the dimer unit. The adenosine portion of FAD is located at the subunit interface of the dimer unit. FAD is enclosed inside the protein with three percent of the molecular surface of FAD solvent accessible.

The anionic 3S-C8-CoA interacts with the monomer of the dimer unit. The binding site for 3S-C8-CoA is formed at the interface between the β-domain and the C-terminal α-domain with the terminal acyl group encapsulated within the tunnel formed at the interface between the N- and C-terminal α-domains (Fig. 4a).

Active Site Structure—The active site structure of 3S-C8-CoA-MCAD is shown in Fig. 4b. The fatty acyl end and thioester region of the anionic 3S-C8-CoA are located in the deep cleft of MCAD with the plane formed by the S1, C1, O1, C2, and S3 atoms facing the *re*-face of the flavin ring. The plane is parallel to the flavin ring and the perpendicular distance between the two planes is 3.3 Å. The catalytic base Glu376-COO^-, which eliminates the α-proton [C(2)-H] of 3S-C8-CoA, is surrounded by hydrophobic Leu103, Phe252, and Val259, the hydrophobic portion of Arg256, and the neutral Thr255 and Tyr375.

The binding of 3S-C8-CoA or C8-CoA liberates three water molecules coordinated to the γ-carboxylate of the catalytic base in the native form (*3*). The liberation of these water molecules from the active site further increases the hydrophobicity around the γ-carboxylate, although the γ-carboxylate changes its side-chain direction to form a new hydrogen bond with the OH group of Thr255. The hydrophobic environment raises the *p*Ka value of the side-chain carboxyl group of Glu376 to reinforce its capability as the catalytic base. Interestingly, a weak electrostatic interaction is observed between Glu376 and Arg256 in the ligand-free form of MCAD (*3*) since the carboxylate of Glu376 is at a distance of 4.3 Å from the guanidino group of Arg256 (Fig. 5). The binding of 3S-C8-CoA to MCAD induces the side-chain rearrangement of Glu376 and Arg256 to lengthen the distance from 4.3 to 4.8 Å. This lengthening should contribute, at least partly, to the rise in the *p*Ka value of Glu376-COOH. The rearranged guanidino group of Arg256 in turn forms a hydrogen bond with the terminal carbonyl group of pantothenate in 3S-C8-CoA. The side-chain movement of Arg256 induced by the approach of 3S-C8-CoA to the active site may play an important role in the catalytic action of the enzyme by raising the *p*Ka value of the carboxylate of Glu376 and stabilizing the MCAD complex with 3S-C8-CoA by hydrogen bond formation.

The carboxylate of Glu376 is at a distance of 4.9 Å from the Cα atom of the anionic 3S-C8-CoA, which seems too long for Glu376 to abstract the α-proton. When the 3S-C8-CoA was modeled into the active site of the native MCAD (*3*) by superposing the 3S-C8-CoA-MCAD structure onto that of the native MCAD, the distance between the carboxylate of Glu376 and Cα atom of the introduced 3S-C8-CoA is 2.6 Å, implying that upon the entry of 3S-C8-CoA into the active site, Glu376-COO^- eliminates the α-proton of the approaching 3S-C8-CoA by liberating water molecules hydrogen-bonded to Glu376-COO^-. After α-proton elimination, Glu376 changes its side-chain direction to interact with Thr255.

Interaction between FAD and 3S-C8-CoA—The 3S-C8-CoA is a substrate analog in which the β-methylene group [C(3)H_2] of the substrate, octanoyl-CoA (C8-CoA), is replaced by a sulfur atom (S3). The 3S-C8-CoA binds to the oxidized form of MCAD to form a charge transfer complex characterized by a broad and intense absorption band with a peak at 808 nm (Fig. 6). The α-proton of 3S-C8-CoA bound to the active site is eliminated by the catalytic base (Glu376-COO^-) as in the reaction with a natural substrate (*4*). The negative charge produced at the C2 atom is delocalized to O1 through the conjugated π-system comprising p-orbitals of the C1, O1, and C2 atoms. The reaction freezes at this stage since the β-hydrogen [C(3)-H], which would be transferred to the flavin ring as a hydride, is absent (*6*). If dehydrogenation of a natural susbtrate, acyl-CoA, by MCAD is stepwise with α-proton elimination preceding β-hydride transfer, then this

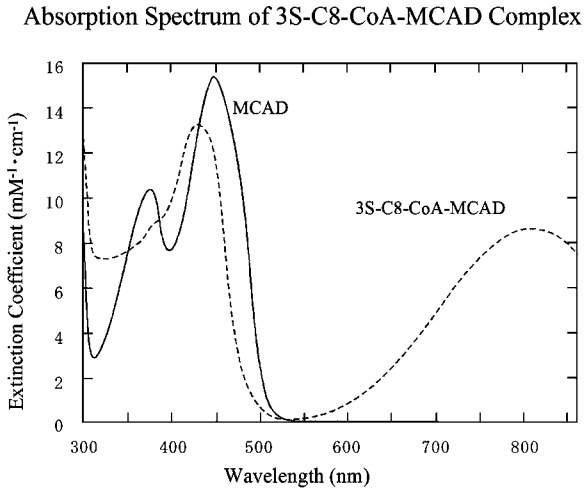

Fig. 6. **Absorption spectra of MCAD in the absence and the presence of 3S-C8-CoA at pH 7.8 and 25°C with a light path of 1cm.** Concentrations were: MCAD, 33 μM; 3S-C8-CoA, 770 μM.

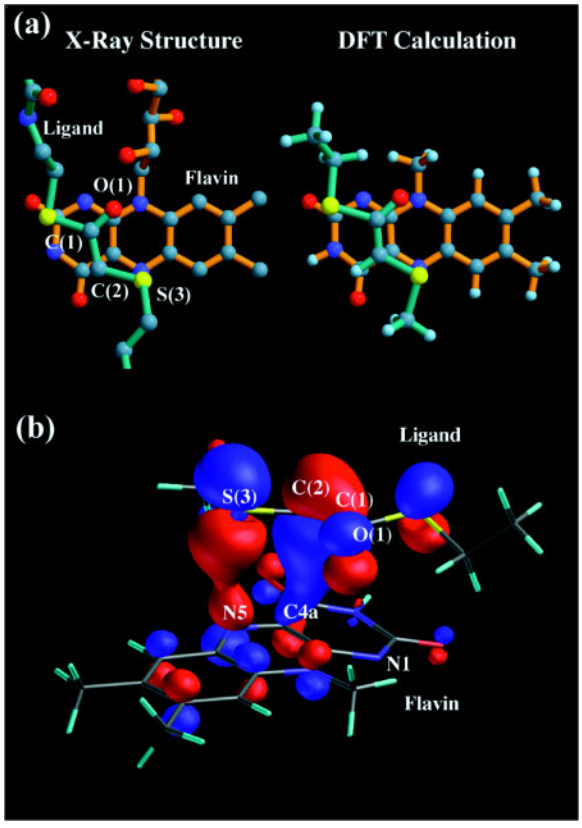

Fig. 7. **(a) The alignment of the anionic ligand with respect to the flavin ring.** X-ray structure of MCAD in complex with 3S-C8-CoA (left). The optimized structure of the complex between lumiflavin and deprotonated 3-thiobutanoic acid ethylthioester (right). **(b) Highest occupied molecular orbital of the complex model between lumiflavin and deprotonated 3-thiobutanoic acid ethylthioester.**

charge-transfer complex between anionic 3S-C8-CoA indeed mimics the metastable intermediate immediately before the β-hydride transfer. If, on the other hand, dehydrogenation of acyl-CoA by MCAD is a concerted process comprising α-proton abstraction and β-hydride transfer, then the charge-transfer complex in question strongly reflects the electronic state of the transition state as described below. In the transition state of the concerted process, the negative charge on the catalytic base, Glu376-COO^-, is delocalized through H-Cα-Cβ-H toward N(5) of flavin. This delocalization is intrinsically of the charge-transfer nature. The charge transfer complex therefore corresponds to the intermediary state during the process of α-proton elimination and β-hydride transfer to the flavin ring, whether the catalysis with natural substrate is stepwise or concerted. This indicates that the complex is a unique and excellent transition-state analog and the detailed structural information obtained herein on the alignment between the ligand and flavin, therefore, is invaluable for understanding the transition state in the reaction of MCAD with a natural substrate.

The plane formed by S1, C1, O1, C2, and S3 of the anionic 3S-C8-CoA as the electron donor stacks on the flavin ring of FAD, the electron acceptor, in a parallel fashion. Fig. 7a (left) is a view perpendicular to these two planes. The complex is characterized by an anionic delocalized π-system (C2, C1, and O1) lying on the pyrimidine ring of FAD. The C1-C2 bond of 3S-C8-CoA, which has a partial double bond character, is nearly parallel to the C4a–C10a bond with C1 and C2 projected onto the pyrimidine ring and the midpoint of the C4-C4a bond, respectively. The remaining S1, O1, and S3 atoms overlap on C2, C10a, and N5 of the flavin ring, respectively.

In order to confirm and exemplify the charge transfer interaction between anionic 3S-C8-CoA and the flavin ring, molecular orbital calculations were carried out on the complex model between lumiflavin and 3-thiabutanoic acid ethylthioester in its C(2)-deprotonated form using the Gaussian98 program (*20*) (see "MATERIALS AND METHODS"). Lumiflavin and the S1, C1, O1, C2 and S3 atoms of the anionic ligand in the calculated theoretical complex model [Fig. 7a (right)] were fitted to the corresponding portion of the X-ray structure with an rms deviation of 0.222, 0.297, and 0.286 Å for subunits a, b, and c, respectively, by the least-squares method. The relative orientation between the flavin ring and the anionic ligand observed in the crystal structure of 3S-C8-CoA-MCAD was indeed reproduced by the molecular orbital calculation, indicating that the theoretical treatment based on the molecular orbital calculations is justified for understanding the interaction between the anionic 3S-C8-CoA and FAD in relation to MCAD catalysis.

The HOMO (highest occupied molecular orbital) of the complex model is given in Fig. 7b showing from which site of the anionic ligand to which site of lumiflavin in the oxidized form electron flow occurs. Two large orbital contributions located between the two planar groups of the complex model range from the anionic ligand to the flavin ring system of lumiflavin. One extends from the C(1)–C(2) region to C(4a) and the other extends from S(3) to N(5). The negative charge on the anionic ligand is thus mainly transferred from C(1)–C(2) to C(4a), and, appreciably, from S(3) to N(5). A large amount of negative charge (0.37 e) on the anionic ligand was calculated to migrate into lumiflavin in the oxidized form (see "MATERIALS AND

METHODS") and the charge-transfer nature of this complex was theoretically confirmed. This electron transfer resulting from the delocalization of the negative charge produces a large stabilization energy (9.2 kcal/mol) of the complex model in comparison with the free anionic ligand and lumiflavin.

The charge transfer interaction as large as 9.2 kcal/mol should play an important role in determining the detailed location of the S1, C1, O1, C2, and S3 region of the anionic 3S-C8-CoA with respect to the flavin ring of FAD. On the basis of the nature of the 3S-C8-CoA-MCAD complex as a transition-state analog, this notion can be extended to the enzyme-substrate complex. Namely, the electron transfer from the anionic substrate to the flavin ring is reasonably assumed to occur as shown by the molecular orbital calculation on the complex model since the theoretical structure of the complex model is essentially the same as that of the corresponding part of the X-ray structure (Fig. 7a). We have thus integrated structural information of the transition state analog into the theoretical treatment of the interaction between the intermediate state of substrate and flavin. The appreciable contribution of S(3)···N(5) in the HOMO of the model complex, the transition-state analog, together with the geometrical proximity of S3 to N(5) of flavin are strongly indicative of hydride-transfer from C(3)-H to flavin N(5) coupled with the α-proton abstraction in the MCAD catalysis. Thus our treatment described in this report theoretically substantiates the α-proton abstraction/β-hydride transfer hypothesis that was proposed based primarily on kinetic analysis (*2*, *4*). We are encouraged by the success of our theoretical treatment and convinced of the validity of the density functional theory method employed to MCAD catalysis. Our next goal is to apply this method to the entire process of MCAD reaction, integrating the structural details into the calculation with a suitable model set for each elementary step. Such treatment will eventually resolve the stepwise/concerted issue of MCAD catalysis and will integrate the stepwise and concerted processes in a generalized form for the reaction catalyzed by the members of the acyl-CoA dehydrogenase family.

We thank Dr. Yasuo Musashi, Kumamoto University Center for Multimedia and Information, for allowing us to use the HP Exemplar Technical Server V2250K computer. This study was supported in part by the following grants: Grant-in-Aid for Scientific Research on Priority Areas from the Ministry of Education, Science, Sports, and Culture of Japan [13125207 (K.H.) and 13125206 (R.M.)], Research Grant from the Japan Society for the Promotion of Science [13480196(K.H.) and 13680745(H.T.)], and National Project on Protein Structural and Functional Analyses. Coordinates for medium-chain acyl-CoA dehydrogenase complexed with 3-thiaoctanoyl-CoA have been deposited in the RSCB Protein Data Bank as entry 1UDY.

REFERENCES

1. Crane, F.L., Mii, S., Hauge, J.G., Green, D.E., and Beinert, H. (1956) On the mechanism of dehydrogenase of fatty acyl derivatives of coenzyme A. I. The general fatty acyl coenzyme A dehydrogenase. *J. Biol. Chem.* **218**, 701–716
2. Engel, P.C. (1992) Acyl-CoA dehydrogenases in *Chemistry and Biochemistry of Flavoenzymes*. (Müller, F., ed.) Vol. III, pp. 597–655, CRC Press, Boca Raton, Ann Arbor, London
3. Kim, J.J.-P, Wang, M., and Paschke, R. (1993) Crystal structures of medium-chain acyl-CoA dehydrogenase from pig liver mitochondria with and without substrate. *Proc. Natl Acad. Sci. USA* **15**, 7523–7527
4. Ghisla, S., Thorpe, C., and Massey, V. (1984) Mechanistic studies with general acyl-CoA dehydrogenase and butyryl-CoA dehydrogenase: Evidence for the transfer of β-hydrogen to the flavin N(5)-position as hydride. *Biochemistry* **23**, 3154–3161
5. Lau, S.M., Brantley, R.K., and Thorpe, C. (1988) The reductive half-reaction in Acyl-CoA dehydrogenase from pig kidney: studies with thiaoctanoyl-CoA and oxaoctanoyl-CoA analogues. *Biochemistry* **27**, 5089–5095
6. Tamaoki, H., Nishina, Y., Shiga, K, and Miura, R. (1999) Mechanism for the recognition and activation of substrate in medium-chain acyl-CoA dehydrogenase. *J. Biochem.* **125**, 285–296
7. Gorelick, R.J., Mizzer, J.P., and Thorpe, C. (1982) Purification and properties of electron-transferring flavoprotein from pig kidney. *Biochemistry* **21**, 6936–6942
8. Lau, S.-M., Powell, P., Buettner, H., Ghisla, S., and Thorpe, C. (1986) Medium-chain acyl coenzyme A dehydrogenase from pig kidney has intrinsic enoyl coenzyme A hydratase activity. *Biochemistry* **25**, 4184–4189
9. Jancarik, J. and Kim, S.-H. (1991) Sparse matrix sampling: a screening method for crystallization of proteins, *J. Appl. Crystallogr.* **24**, 409–411
10. Matthews, B.W. (1968) Solvent content of protein crystals. *J. Mol. Biol.* **33**, 491–497
11. Otwinowski, Z. (1993) Data collection and processing in *Proceedings of the CCP4 Study Weekend*, pp.56–62, SERC Daresbury Laboratory, Warrington
12. Navaza, J. (1994) AMoRe: an automated package for molecular replacement. *Acta Crystallogr.* **A50**, 157–163
13. Kim, J.-J.P. and Wu, J. (1988) Structure of the medium-chain acyl-CoA dehydrogenase from pig liver mitochondria at 3-Å resolution. *Proc. Natl Acad. Sci. USA* **85**, 6677–6681
14. Brunger, A.T., Adams, P.D., Clore, G.M., DeLano, W.N., Gros, P., Grosse-Kunstleve, R.W., Jiang, J.-S., Kuszewski, J., Nilges, M., Pannu, N.S., Read, R.J., Rice, L.M., Simonson, T., and Warren, G.L. (1998) Crystallography & NMR System: A New Software Suite for Macromolecular Structure Determination, *Acta Crystallogr.* **D54**, 905–921
15. Jones, T.A., Zou, J.-Y., Cowan, S.W., and Kjeldgaard, M. (1991) Improved methods for building protein models in electron density maps and the location errors in these models. *Acta Crystallogr.* **A47**, 110–119
16. Laskowski, R.A., MacArthur, M.W., Moss, D.S., and Thornton, J.M. (1993) PROCHECK: a program to check the stereochemical quality of protein structures. *J. Appl. Crystallogr.* **26**, 283–291
17. Kraulis, P.J. (1991) MOLSCRIPT: a program to produce both detailed and schematic plots of protein structures. *J. Appl. Crystallogr.* **24**, 946–950
18. Esnouf, R.M. (1997) An extensively modified version of Molscript that includes greatly enhanced coloring capabilities. *J. Mol. Graphics.* **15**, 132–134
19. Merritt, E.A. and Murphy, M.E.P. (1994) Raster3D version 2.0: a program for photorealistic molecular graphics. *Acta Crystallogr.* **D50**, 869–873
20. Frisch, M.J., Trucks, G.W., Schlegel, H.B., Scuseria, G.E., Robb, M.A., Cheeseman, J.R., Zakrzewski, V.G., Montgomery, Jr., J.A., Stratmann, R.E., Burant, J.C., Dapprich, S., Millam, J.M., Daniels, A.D., Kudin, K.N., Strain, M.C., Farkas, O., Tomasi, Barone, J.V., Cossi, M., Cammi, R., Mennucci, B., Pomelli, C., Adamo, C., Clifford, S., Ochterski, J., Petersson, G.A., Ayala, P.Y., Cui, Q., Morokuma, K., Malick, D.K., Rabuck, A.D., Raghavachari, K., Foresman, J.B., Cioslowski, J., V. Ortiz, J., Stefanov, B.B., Liu, G., Liashenko, Piskorz, A.P., Komaromi, I., Gomperts, R., Martin, R.L., Fox, D.J., Keith, T.,

Al-Laham, M.A., Peng, C.Y., Nanayakkara, A., Gonzalez, C., Challacombe, M., Gill, P.M.W., Johnson, B., Chen, W., Wong, M.W., Andres, J.L., Gonzalez, C., Head-Gordon, M., Replogle, E.S., and Pople, J.A. (1998) *Gaussian* **98**, *Revision A.7* Gaussian, Pittsburgh PA
21. Becke, A.D. (1993) Density-functional thermochemistry. III. The role of exact exchange. *J. Chem. Phys.* **98**, 5648–5652
22. Lee, C., Yang, W., and Parr, R.G. (1988) Development of the Colle-Salvetti correlation-energy formula into a functional of the electron density. *Phys. Rev.* **B37**, 785–789
23. Mulliken, R.S. (1955) Electronic population analysis on LCAO-MO molecular wave functions. *I. J. Chem. Phys.* **23**, 1833–1840
24. Foresman, J.B. and Frisch, AE. (1996) *Exploring Chemistry with Electronic Structure Methods*, 2nd ed., pp. 194–197, Gaussian, Pittsburgh, PA